

Regional Features of Water Density Stratification and Internal Wave Characteristics in the Arctic Seas

A. A. Bukatov, N. M. Solovei, E. A. Pavlenko

Marine Hydrophysical Institute of RAS, Sevastopol, Russian Federation

✉ nele7@mail.ru

Abstract

Purpose. The work is purposed at summarizing the results of studies both of the spatio-temporal variability of water density stratification and the internal wave characteristics in the Barents, Kara, Laptev, East Siberian, Chukchi and Beaufort seas.

Methods and Results. Based on the *World Ocean Atlas* data, the average monthly profiles of buoyancy frequency were calculated at the $0.25^\circ \times 0.25^\circ$ grid points for 1959–2020. To study the vertical structure and dispersion characteristics of internal waves, the eigenvalues and eigenfunctions of the main boundary value problem of the Sturm – Liouville type were found at the fixed values of a wave number. The regional features of vertical structure and intra-annual variability of the Väisälä – Brunt frequency were revealed. The relationship between the water density vertical structure and the free internal wave characteristics in the seas under consideration was analyzed.

Conclusions. It is shown that maximum water stability in the Barents Sea takes place in July – August, in the Kara Sea – in September and November, in the Laptev Sea – from June to November, in the East Siberian and Chukchi seas – in July, and in the Beaufort Sea – in June. In the same months, the smallest values of the amplitude of vertical velocity component as well as the smallest own periods of internal waves are noted. The depth of maximum values of the vertical component amplitude of internal wave velocities exceeds that of the density gradient maximum values by about 10–20 m.

Keywords: Barents Sea, Kara Sea, Laptev Sea, East Siberian Sea, Chukchi Sea, Beaufort Sea, Väisälä – Brunt frequency, internal waves, first mode, amplitude of velocity vertical component, own frequency, own period

Acknowledgements: The investigation was carried out within the framework of state assignment on theme FNNN-2021-0004.

For citation: Bukatov, A.A., Solovei, N.M. and Pavlenko, E.A., 2023. Regional Features of Waters Density Stratification and Internal Wave Characteristics in the Arctic Seas. *Physical Oceanography*, 30(6), pp. 731-746.

© 2023, A. A. Bukatov, N. M. Solovei, E. A. Pavlenko

© 2023, Physical Oceanography

Introduction

The water structure of the Arctic seas is formed as a result of interaction of the Central Polar Basin waters, Atlantic waters brought by the warm Gulf Stream, Pacific waters entering through the Bering Strait and waters of continental runoff.

Warm and salty Atlantic waters enter the Arctic Region through two main branches, each representing a flow of 2 Sverdrups (Sv) ($\sim 60,000 \text{ km}^3/\text{year}$): the Fram Strait branch (West Spitsbergen Current) and the Barents Sea branch (North Cape Current) [1, 2]. Through deep-sea trenches, Atlantic waters penetrate into the Arctic seas far to the east. The annual volume of Pacific waters entering



the Chukchi Sea through the Bering Strait is ~ 1 Sv [3]. Traces of Pacific waters are found off the coast of Greenland, from where they are removed from the Arctic basin in a transformed form ¹.

The Arctic Ocean is the smallest of the oceans, but it receives the largest amount of fresh water brought by the rivers of Eurasia and America. River waters, entering the Arctic seas, propagate in a thin layer over their surface and mix with salty sea waters. In the process of interaction of fresh waters with more saline deep waters, significant vertical density gradients are formed ¹. The largest rivers that make the main contribution to the Arctic Ocean salt balance are the Pechora (113 km³/year), the Ob (406 km³/year), the Yenisei (607 km³/year), the Khatanga (87 km³/year), the Lena (556 km³/year), the Kolyma (103 km³/year), the Mackenzie (285 km³/year) and the Yukon (203 km³/year). Although the Yukon flows into the Bering Sea, most of its runoff together with the Alaska Coastal Current enters the Chukchi Sea ² [4].

Density stratification can be represented by a buoyancy frequency profile (Väisälä – Brunt), which helps to estimate the location of the density transition zone (pycnocline), the boundaries of water masses of various origins, the convection distribution depth, etc. The vertical structure of waters is also closely related to the functioning features of aquatic ecosystems. For example, the main accumulations of zooplankton, which is a food source for most pelagic fish, coincide in vertical distribution with the pycnocline depth. The density stratification causes formation of internal waves (IW), which are an important factor in the formation of vertical and horizontal water circulation. These types of fluid movement contribute to the exchange of energy, mixing and enrichment with oxygen as well as supply of nutrients from the depths.

This paper focuses on the study of density structure of waters in the Arctic seas, characteristics of internal waves, their relationships and includes a generalization of the results obtained in [4, 5–10].

Materials and methods

Temperature and salinity values from WOA-2018 at $0.25^\circ \times 0.25^\circ$ grid nodes for the period 1959–2020 were used as input hydrological data [11, 12]. The study area is limited by parallels 65° N and 80° N and meridians 16° E and 120° W. For each grid node, the average monthly Väisälä – Brunt frequency profiles (N , cycle/h) were calculated using the following formula:

$$N^2(z) = \frac{g}{\rho} \frac{d\rho}{dz},$$

where z is depth; g is gravitational acceleration; ρ is density. The Väisälä – Brunt frequency maximum in depth ($N_{\max}(z)$, cycle/h) and its occurrence depth ($HN_{\max}(z)$, m) were determined.

¹ Nikiforov, E.G. and Shpayher, A.O., 1980. [Patterns of Formation of Large-Scale Fluctuations of the Hydrological Regime of the Arctic Ocean]. Leningrad: Gidrometeoizdat, 270 p. (in Russian).

² Holmes, R.M., McClelland, J.W., Tank, S.E., Spencer, R.G.M. and Shiklomanov, A.I., 2021. Arctic Great Rivers Observatory IV Biogeochemistry and Discharge Data: 2020–2024: Discharge Dataset. Arctic Data Center. Version 20220630. doi:10.18739/A2FQ9Q683

The study of internal waves was carried out based on a system of linear equations of motion of a continuously stratified fluid in the Fjeldstad form, which has a solution in the form of a superposition of plane waves ³. In particular, for the velocity vertical component $w(x, y, z, t)$ (x, y are horizontal coordinates, t is time) we have the following representation:

$$w(x, y, z, t) = \sum_{n=1}^{\infty} \int_{-\infty}^{\infty} \int_{-\infty}^{\infty} W^{(n)}(k, z) \exp\{i [k_x x + k_y y - \omega^{(n)}(k) t]\} dk_x dk_y,$$

where $\omega^{(n)}(k)$ is dispersion relation (own frequency) for a mode with number n and wave number $k = (k_x^2 + k_y^2)^{1/2}$; $W^{(n)}(k, z)$ is amplitude of this mode (own function).

If we use the Boussinesq approximation, filter out surface waves and neglect the Earth rotation, then $W^{(n)}(k, z)$ will be a solution to a boundary value problem of the Sturm – Liouville type with zero boundary conditions at the bottom and free surface of the liquid [8]:

$$d^2 W^{(n)} / dz^2 + (\lambda^{(n)} N^2 - k^2) W^{(n)} = 0, \quad W^{(n)}(H) = W^{(n)}(0) = 0,$$

where $\lambda^{(n)} = (k / \omega^{(n)})^2$ is own value; H is depth.

This spectral problem corresponds to determining the own values $\lambda^{(n)}$ and own functions $W^{(n)}(k, z)$ for each fixed value of the wave number. For the numerical implementation of the boundary value problem for a given profile $N(z)$, its finite-difference approximation was constructed. The resulting system of linear algebraic equations was solved by finding the roots of the characteristic equation of its matrix [8, 9, 13].

To study the vertical structure and dispersion properties of IW, the own values and own functions were calculated for wavelengths > 200 m. When choosing the wavelength interval, the authors turned to works [14–16] maintaining that at high latitudes in radar images the internal waves with lengths of 200–3000 m are observed. As an illustration, the distributions of IW characteristics for a wavelength (λ) of 1000 m are given in the paper.

The first mode is dominant in the wave train spectrum [17], therefore, in this work, we calculated the characteristics of the first mode of free internal waves (the amplitude k of the vertical velocity component ($W^{(1)}(k, z)$ in dimensionless units) and own periods ($T^{(1)}(k)$ in hours, minutes)).

Analysis of results

The seas of the Arctic Ocean are marginal ones. They are limited by the coasts of the continents in the south and they freely interact with the ocean in the north. They are separated by conventional lines and islands and connected by straits. In addition, large rivers flow into almost all the seas.

³ Miropol'sky, Yu.Z., 2001. *Dynamics of Internal Gravity Waves in the Ocean*. Atmospheric and Oceanographic Sciences Library, vol. 24. Dordrecht: Springer Science + Business Media, 406 p. doi:10.1007/978-94-017-1325-2

The Barents and Kara seas. These are the western seas of the Russian Arctic, which are separated by the Novaya Zemlya archipelago. The hydrological regime of the seas is formed under the effect of Arctic, Atlantic and river waters. In the Barents Sea, there is a complex circulation system associated with the North Atlantic Current and its branches (Murmansk, Novaya Zemlya, Perseus, Barents, Medvezhinskoe, etc.). As a result of their interaction, a cyclonic circulation is formed, where warm Atlantic waters mix with cold runoff waters of the Arctic Ocean [5, 18]. The warmer and saltier Barents Sea waters penetrate into the Kara Sea through the Yugorsky Strait, Kara Strait, and Matochkin Strait, which, together with the Eastern Novaya Zemlya and Yamal currents as well as the western branch of the Ob-Yenisei Current, also form a well-defined cyclonic gyre in the southwest and a less distinct one in the north of the sea.

The river runoff into the Barents Sea is small, its maximum is observed in late spring – early summer. The Kara Sea accounts for ~55% of the total coastal runoff to all Siberian seas; the maximum river water is observed in late summer – early autumn ⁴[5]. The Ob and Yenisei flow into the Kara Sea through estuaries, where river waters interacting with sea waters form a river plume, which extends hundreds of kilometers from the point where the river flows into the sea and has a significant impact on processes in the active layer [19]. Saltier and warmer Atlantic waters penetrate into the Kara Sea northern region along the St. Anna and Voronin troughs between Franz Josef Land and Novaya Zemlya [20].

In the cold months of the year, stability of waters in the Barents Sea is low or close to unstable [5, 21]. The criterion for the vertical stability of layers in the sea is the vertical density gradient value inclusive of the adiabatic correction [21]. At depths up to ~ 1000 m, this correction can be neglected due to its smallness, and the buoyancy frequency can be considered instead of the density gradient. The geographic distribution of $N_{\max}(z)$ and $HN_{\max}(z)$ in the Barents and Kara seas in July is represented in Fig. 1, 2. It can be seen that in July the waters with maximum stability are located in coastal areas: in the area of the Pechora River delta (Pechora Sea, ~ 50 cycle/h), the coast of the Yamal Peninsula, in the estuary areas of the Ob and Yenisei (~ 60–70 cycle/h). The central part of the Barents Sea is occupied by the waters with low values of $N_{\max}(z)$ (< 7 cycle/h). Northwards of the 75th parallel, the maximum buoyancy frequency increases to 10–15 cycle/hour. In the central part of the Kara Sea from 75° N to 80° N, $N_{\max}(z)$ values are ~ 20 cycle/h, to the south – ~ 80 cycle/h; in the southwestern part of the Kara Sea the values are 30–50 cycle/h. High stability in the southeastern part of the Barents Sea and the southern part of the Kara Sea is due to the influx of fresh continental waters, which increases the salinity gradient in the coastal zone. Surface heating also creates a temperature gradient at this time of year, but its impact on the stability compared to the salinity gradient is less significant [5, 22]. In July, a relatively high stability of waters in the Barents Sea northwards of 75° N is caused by the salinity gradient increase due to the melting ice. The low stability in the central part (isoline $N_{\max}(z)$ ~ 7 cycle/h) is caused by the presence of Atlantic waters (North Cape Current), which have high

⁴ Dobrovolsky, A.D. and Zalogin, B.S., 1982. *Seas of the USSR*. Moscow: MSU, 192 p. (in Russian).

salinity and temperature (Fig. 1). As they move eastward, they mix with the Barents Sea waters, cool down and descend from the surface to the layer of higher density. This leads not only to a decrease in water stability, but also, as a consequence, to a deepening of the Väisälä – Brunt frequency maximum to 40 m (Fig. 2) [21]. Small values of the maximum buoyancy frequency in the center of the Kara Sea eastern part in July are most likely due to the slow movement of desalinated coastal waters to the north.

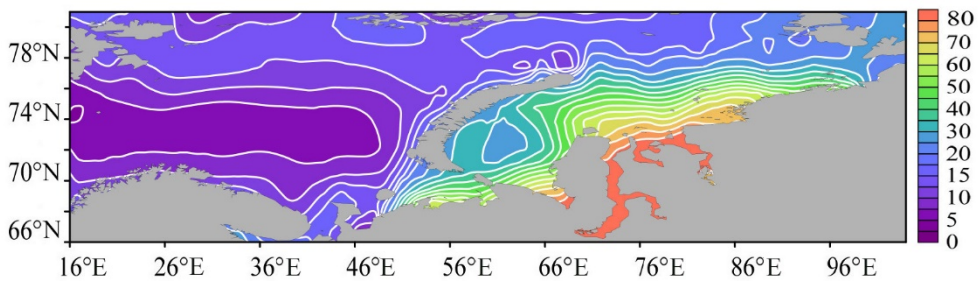


Fig. 1. Average long-term distribution of the Väisälä – Brunt frequency maximum (cycle/hour) in the Barents and Kara seas in July

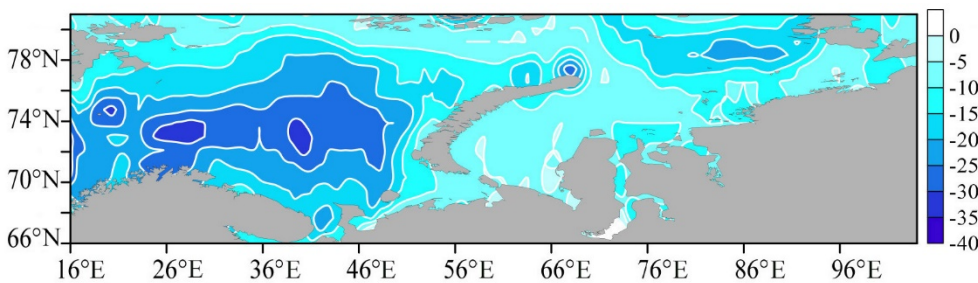


Fig. 2. Average long-term distribution of the Väisälä – Brunt frequency maximum depth (m) in the Barents and Kara seas in July

To characterize intra-annual variability of water stability in the Arctic seas, average values of Väisälä – Brunt maximum frequency ($N_{\max}(z)_{\text{average}}$) (Fig. 3, *a*) and average depths of their occurrence ($HN_{\max}(z)_{\text{average}}$) (Fig. 3, *b*) were calculated for each month. The average values were obtained as arithmetic averages over the entire sea area. It can be seen that maximum stability in the Barents Sea occurs in July – August and in the Kara Sea – in August – September and November. In October, stability in the Kara Sea decreases with the beginning of ice formation process. In November, river waters begin to propagate into subglacial horizons with the formation of ice cover, which leads to stability increase [5, 22]. In the warm season, the density transition zone rises to the surface and in winter it goes deeper. In the Barents Sea, the average depth of pycnocline is ~ 24 m in summer and ~ 60 m in winter, in the Kara Sea, the average depth of pycnocline is ~ 14 m in summer and ~ 35 m in winter (Fig. 3, *a, b*).

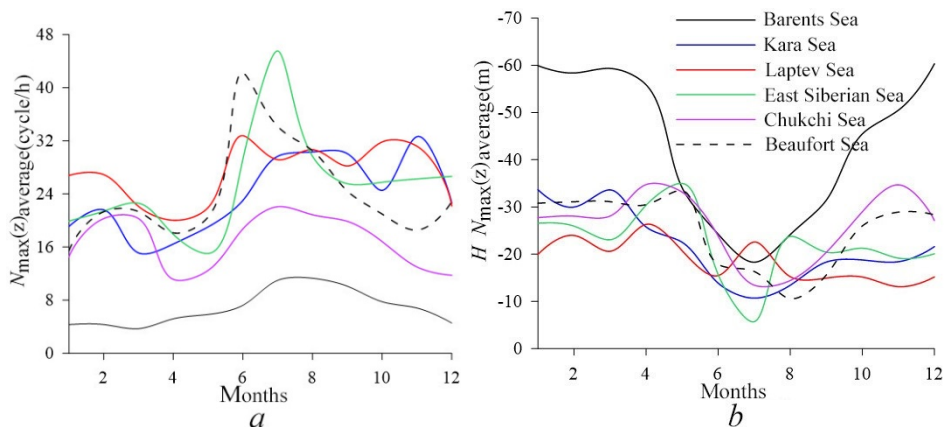


Fig. 3. Intra-annual variation of the sea area average value of $N_{\max}(z)$ (a) and its depths (b)

The Laptev and East Siberian seas. The hydrological conditions of the Laptev Sea and the East Siberian Sea are formed mainly under the effect of interaction of the surface Arctic waters and the river ones. The coastal runoff into the Laptev Sea is $\sim 30\%$ of the total volume of the continental runoff into all seas of the Russian Arctic, and into the East Siberian Sea $\sim 10\%$ ⁴. The Lena carries its waters into the Laptev Sea through narrow and shallow branches forming a wide delta. Fresh river waters overlap salty and dense sea waters propagating over them in a thin layer. The resulting river plume depends on the wind direction, which is explained by its shallow depth. In years with a predominance of western and northern winds, the desalinated water mass is concentrated in the south of the Laptev Sea and the East Siberian Sea occupying a relatively small area of ~ 250 thousand km^2 and extending less than 250 km to the north. Under the effect of eastern winds, the Lena plume propagates over an area twice as large [19].

In the deep-water areas of the Laptev and East Siberian seas, a layer of saltier and colder water is formed under the surface Arctic waters as a result of interaction of the surface Arctic and deep Atlantic water masses. The vertical structure of waters of the East Siberian Sea northern and eastern parts is formed under the effect of advection of the transformed Pacific waters entering through the Long Strait or along the northern coast of Wrangel Island from the Chukchi Sea ¹ [6].

Density stratification of the Laptev Sea waters is most pronounced from late spring to early autumn. In the zones strongly affected by coastal runoff, the water with a relatively high temperature and low salinity is formed as a result of mixing of river and surface Arctic waters. At their interface (5–10 m horizon), large gradients of salinity and density are formed with maximum values in the southern regions and at the ice edge. At the Lena mouth, $N_{\max}(z)$ values in July reach 80 cycle/h, at the Khatanga mouth – 75 cycle/hour (Fig. 4). In the southeastern part of the Laptev Sea, where most of the Khatanga and Lena runoff propagates under the effect of cyclonic circulation in the sea surface layer, the pycnocline can be traced throughout the year [6]. Wind mixing in the Laptev Sea ice-free areas in summer is weakly developed ¹, which contributes to an increase in the density stratification of waters.

In deeper northern areas, stratification is significantly less during the warm season than in the south. Most of the northern part of the sea is covered with ice and the surface layer warms up weakly.

Surface currents in the Laptev Sea form a cyclonic gyre. Waters moving along the coast from the west to the east involve the Lena runoff. Near the New Siberian Islands, part of the flow deviates to the north and goes beyond the sea, where it connects with the Transpolar Drift Stream. At the Severnaya Zemlya tip, the East Taimyr Current branches off from the formed flow, which moves south along the eastern shores of Severnaya Zemlya and the Taimyr Peninsula, closing the cyclonic ring. Another part of the alongshore current in the Laptev Sea enters the East Siberian Sea through the Sannikov and Dmitry Laptev Straits continuing to move east. Near Wrangel Island, part of the flow turns to the northwest and is carried to the northern edges of the sea connecting with the Transpolar Drift Stream; another part goes into the Chukchi Sea through the Long Strait⁴ [10]. In the East Siberian Sea, the water stratification by density is most pronounced in the south, where desalinated waters of the Siberian Coastal Current as well as waters of the Kolyma and Indigirka rivers enter through the Laptev and Sannikov straits. In this area, the pycnocline can be traced from June to September and by the end of the warm period it is destroyed by wind mixing. In the estuarine areas, $N_{\max}(z)$ values reach 70–85 cycle/h.

The East Siberian Sea is the iciest of the Arctic seas. From October to June, it is completely covered with ice. A significant $N_{\max}(z)_{\text{average}}$ rise in July is apparently associated with an increased ice melting [6, 8]. The intra-annual stability maximum in the southern part of the East Siberian Sea occurs in August, $N_{\max}(z)_{\text{average}}$ is ~ 55 cycle/h at $HN_{\max}(z)_{\text{average}} \sim 5$ m. In the deeper areas of the sea, the intra-annual maximum of water stability occurs in July, $N_{\max}(z)_{\text{average}}$ is ~ 40 cycle/h at $HN_{\max}(z)_{\text{average}} \sim 5$ m (Fig. 4, 5). Large density gradients in the southeastern and northern sea regions are observed throughout the year at 25–55 m depths [6]. These depths correspond to permanent pycnocline layer separating deep waters and surface Arctic or Pacific waters coming from the Chukchi Sea¹. $N_{\max}(z)$ values in the southeastern and northern regions reach ~ 50 cycle/h in the warm period [6, 10].

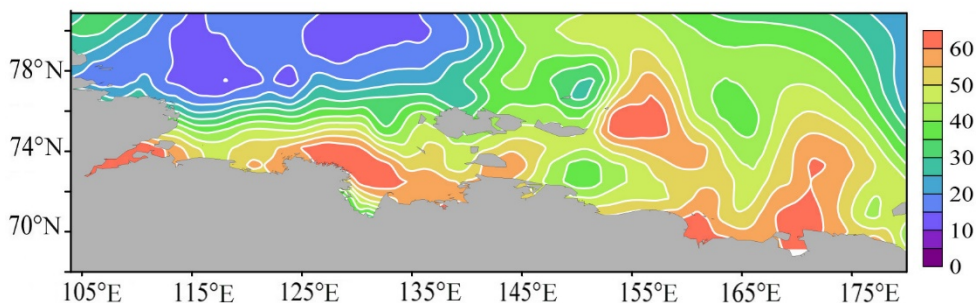


Fig. 4. Average long-term distribution of the Väisälä – Brunt frequency maximum (cycle/hour) in the Laptev and East Siberian seas in July

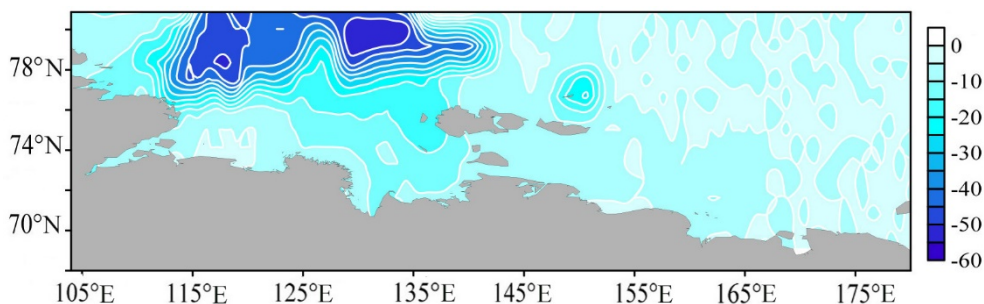


Fig. 5. Average long-term distribution of the Väisälä – Brunt frequency maximum depth (m) in the Laptev and East Siberian seas in July

The Chukchi and Beaufort seas. The Chukchi Sea is the easternmost Eurasian Arctic sea; depths of ~ 50 m prevail in most of its water area. The maximum depths are observed in the north and do not exceed 1300 m. The continental runoff into the Chukchi Sea is small, the total influx of river water⁴ per year is only 72 km³. In this regard, its impact on hydrological conditions is insignificant and affects only the stratification of coastal waters. To a greater extent, the Chukchi Sea hydrological regime is affected by water exchange with the Central Polar Basin and the Pacific Ocean. Pacific waters, flowing out of the Bering Strait into the Chukchi Sea, propagate in different directions. Their main flow is directed northwards. At Kotzebue Sound latitude, they are joined by its waters, freshened by river runoff⁴. Moving further northwards, the Bering Slope Current waters are divided into two streams, one of which in the form of the Alaska Current turns to the northeast; the second deviates to the northwest¹. Moving along the eastern shallow part of the Chukchi Sea shelf with depths of up to 40–50 m, the Bering Sea waters mix with local ones. Therefore, the stratification of waters is expressed relatively weakly here ($N_{\max}(z)$ is ~ 20 cycle/h in July) (Fig. 6) [7]. In the deeper northern regions of the sea, the transformed Pacific waters cool and sink into the subsurface layers forming a layer with a core at 40–100 m horizons, under which deep water is located¹.

A noticeable impact on the hydrological conditions of the Chukchi and Beaufort seas is made by the runoff of rivers flowing into the Laptev and East Siberian seas. The lens formed by the Lena, Yana, Indigirka and Kolyma runoff is the largest in area in the World Ocean [23]. With the intensification of atmospheric cyclonic circulation in the European part of the Arctic, the desalinated and cold waters of the lens flow through the Long Strait with the Siberian Coastal Current into the Chukchi Sea and the Bering Strait. The greatest density stratification is observed at the Chukchi Sea western coast in the area affected by desalinated waters of the Siberian Coastal Current. The buoyancy frequency values reach 50 cycle/hour in July (Fig. 6). With a weak development of the Siberian Coastal Current, the desalinated waters flow northeastwards, reach the Chukchi Sea northern regions and then are drawn into the circulation of the Beaufort Sea increasing the amount of fresh water in this area [7, 23]. In the north of the sea, deep Atlantic waters propagate along the deep-water Chukchi Trough at 400–450 m horizons. These waters enter the Chukchi Sea 5 years after their entry into the Arctic basin near Spitsbergen⁴.

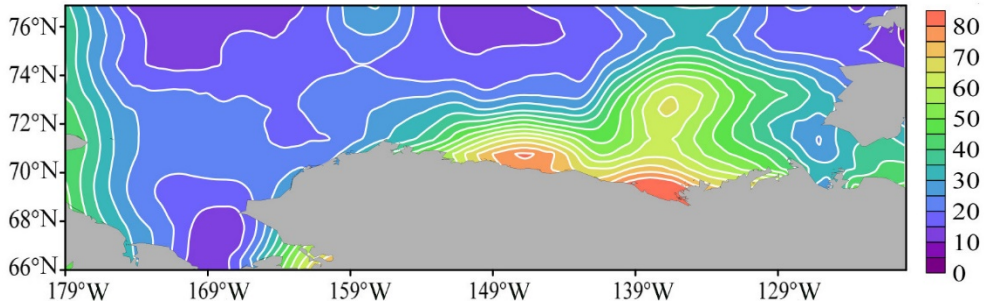


Fig. 6. Average long-term distribution of the Väisälä – Brunt frequency maximum (cycle/hour) in the Chukchi and Beaufort seas in July

The Beaufort Sea is located off the northern coast of Alaska and Canada. Its shelf is the narrowest of all the shelves in the Arctic basin, its width rarely exceeds 50 km. Beyond the shelf, the ocean floor drops sharply forming a basin of more than 3000 m depth. The Beaufort Sea hydrological conditions are determined by its connection with the adjacent regions of the Central Polar Basin, continental runoff (primarily of the Mackenzie River) and the water influx through the Bering Strait. The Beaufort Sea is filled with warm Pacific waters in summer. In the edge areas and in the zone affected by the Mackenzie River runoff, the Pacific waters submerge under the desalinated waters of the Beaufort Sea ¹. Here, the buoyancy frequency values in July reach 80 cycle/h (Fig. 6) at the maximum occurrence depth $N(z)$ 5–10 m (Fig. 7). In the northern part of the Beaufort Sea, on the southern periphery of the Eastern Anticyclonic Gyre of the Central Polar Basin, the maximum density gradients are small (~ 10 – 15 cycle/h); they are observed at ~ 50 – 60 m depths, which corresponds to the depth of the main pycnocline layer. The lowest average values of the maximum buoyancy frequency and the greatest average depths of their occurrence are observed in the cold months. The minimum $N_{\max}(z)_{\text{average}}$ in April is ~ 10 cycle/h at $HN_{\max}(z)_{\text{average}} \sim 35$ m (Fig. 3, *a, b*).

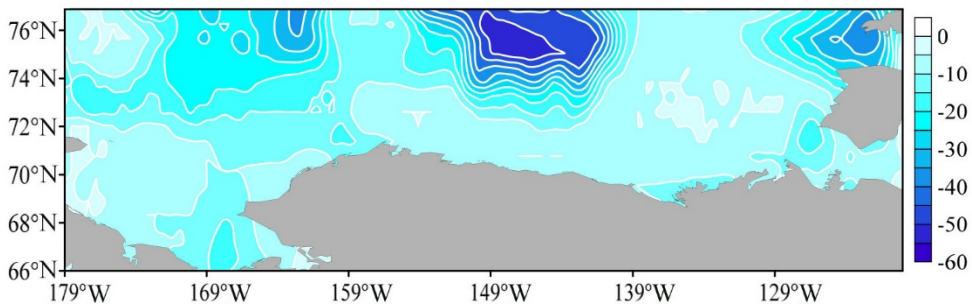


Fig. 7. Average long-term distribution of the Väisälä – Brunt frequency maximum depth (m) in the Chukchi and Beaufort seas in July

Internal waves

The main source of internal wave generation in the ocean is tides. In the Arctic seas, the sources of internal tidal wave generation are localized near the continental

slope and large-scale heterogeneities of bottom topography [24]. Free internal waves of the tidal period propagate throughout the entire thickness of the ocean. However, a latitude close to 74.5° is critical for these IW and northwards of this latitude they cannot exist as free waves. It is believed that in the region of high latitudes the tidal-period internal wave is destroyed as the driving force ends, generating a packet of short-period (high-frequency) waves that have no limitations to exist in polar latitudes. In the Arctic seas located slightly southwards of 74.5°N , the effect of critical behavior of internal waves also takes place. The literature describes a number of experimental observations that confirm the existence of internal short-period waves in the Arctic seas [25].

The intra-annual variation of the IW first mode periods averaged over the sea area is shown in Fig. 8. The period values are presented for a wavelength of 1000 m ($T_{\text{average}}^{(1)}$), however, qualitatively, the graph $T_{\text{average}}^{(1)}(k)$ will have the same form for other wavelengths from the considered range [8, 9]. Fig. 3, a and Fig. 8 show that IW with the shortest periods (highest frequencies) are observed in the months of maximum density gradients. The correlation coefficient (R) between intra-annual cycles $N_{\text{max}(z)}_{\text{average}}$ and $T_{\text{average}}^{(1)}$ is within the range from -0.83 to -0.95 [8]. The shortest-period IW are observed in July – September, during the months of the maximum (summer) water stratification. The minimum $T_{\text{average}}^{(1)}$ value in the Barents Sea is ~ 45 min, in the Kara, Laptev, East Siberian and Chukchi seas ~ 30 min, in the Beaufort Sea ~ 20 min. The maximum values of the averaged own period ($T_{\text{average}}^{(1)\text{max}}$) are observed in winter and spring, when the pycnocline is smoothed everywhere by water mixing ¹. In the Barents Sea, $T_{\text{average}}^{(1)\text{max}}$ is ~ 2 h 20 min, in the Kara and Laptev seas ~ 1 h 10 min, in the East Siberian and Chukchi Seas ~ 1 h 30 min, in the Beaufort Sea ~ 30 min.

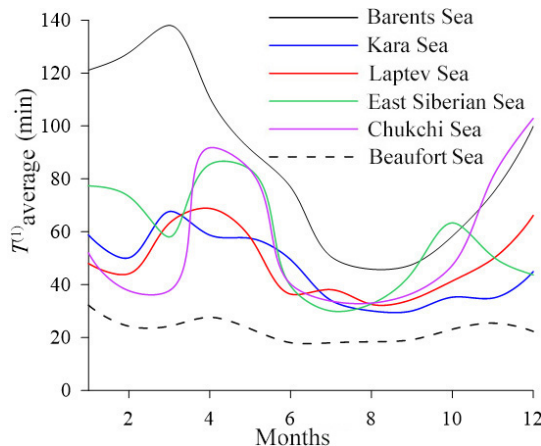


Fig. 8. Intra-annual variation of the sea area average own period of the IW first mode (min), $\lambda = 1000$ m

To analyze IW vertical structure at each grid node, we calculated amplitude profiles of the velocity vertical component of IW first mode, and the maximum $W^{(1)}(z)$ ($W_{\text{max}}(z)$) and its depth ($HW_{\text{max}}(z)$) were determined. Fig. 9–14 present

the long-term average distribution $W_{\max}(z)$ and $HW_{\max}(z)$ in the studied seas in July. The values $W_{\max}(z)$ and $HW_{\max}(z)$ obtained for each month were averaged over sea areas ($W_{\max}(z)_{\text{average}}$, $HW_{\max}(z)_{\text{average}}$) (Fig. 15, *a, b*). It was revealed that the highest values of $W_{\max}(z)_{\text{average}}$ (more intense wave dynamics) are observed in the months of the lowest density gradients: in the Barents and Kara seas – in March, in the Laptev, East Siberian and Beaufort seas – in April, in the Chukchi sea – in April and December. The correlation coefficient between intra-annual cycles $N_{\max}(z)_{\text{average}}$ and $W_{\max}(z)_{\text{average}}$ ranges from -0.73 to -0.95 [8]. In spring and summer, the melting ice and inflowing rivers bring large amounts of fresh water reducing the salinity of the surface layers of the seas and increasing the density gradient in areas of river runoff and ice melting. The minimum amplitude values of the vertical velocity component are also observed there. The desalinated waters form a kind of “a lid” that prevents the mixing of the upper and lower layers and prevents the development of internal waves.

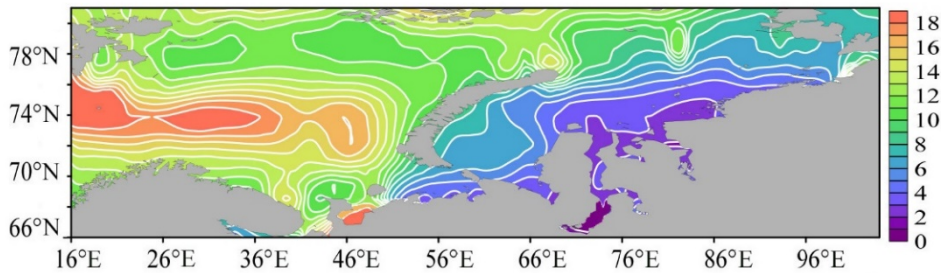


Fig. 9. Average long-term distribution of the maximum amplitude of velocity vertical component of the IW first mode (conventional units) in the Barents and Kara seas in July, $\lambda = 1000$ m

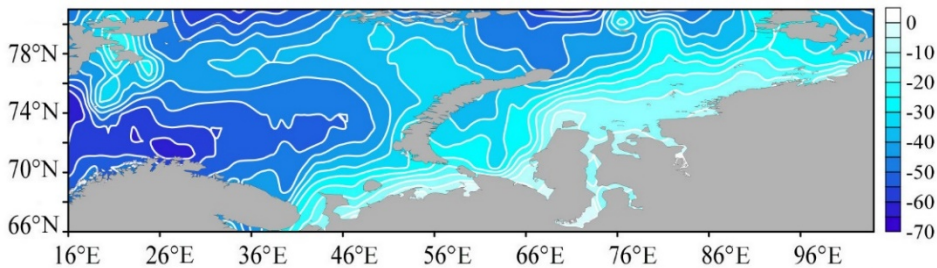


Fig. 10. Average long-term distribution of depth of the maximum amplitude of velocity vertical component of the IW first mode (m) in the Barents and Kara seas in July, $\lambda = 1000$ m

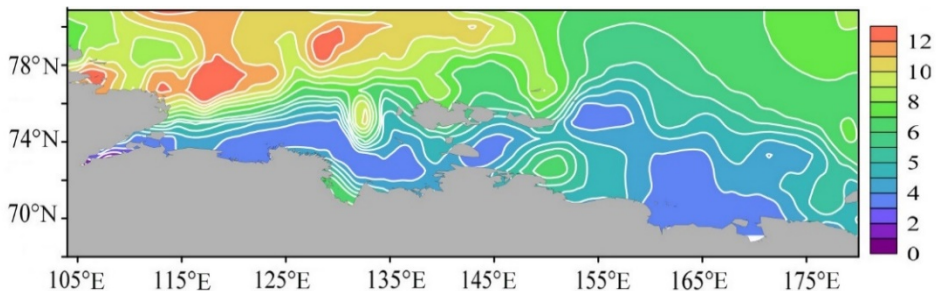


Fig. 11. Average long-term distribution of the maximum amplitude of velocity vertical component of the IW first mode (conventional units) in the Laptev and East Siberian seas in July, $\lambda = 1000$ m

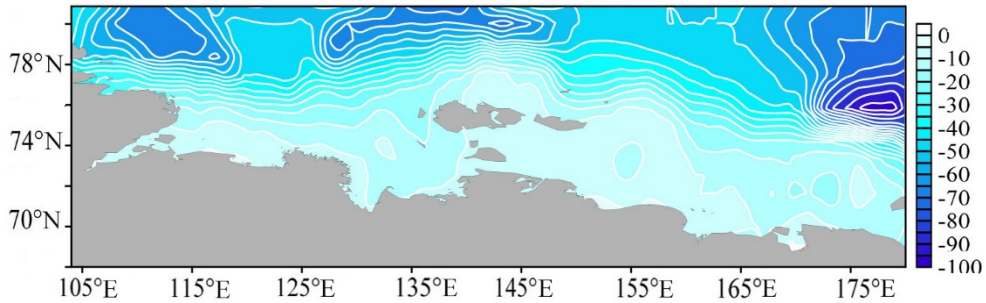


Fig. 12. Average long-term distribution of depth of the maximum amplitude of velocity vertical component of the IW first mode (m) in the Laptev and East Siberian seas in July, $\lambda = 1000$ m

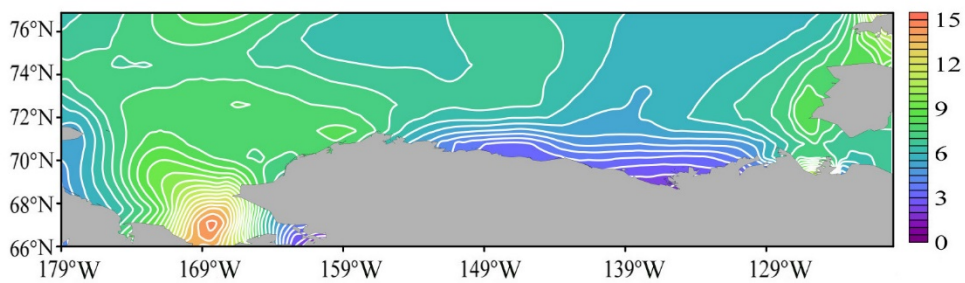


Fig. 13. Long-term average distribution of the maximum amplitude of velocity vertical component of the IW first mode (conventional units) in the Chukchi and Beaufort seas in July, $\lambda = 1000$ m

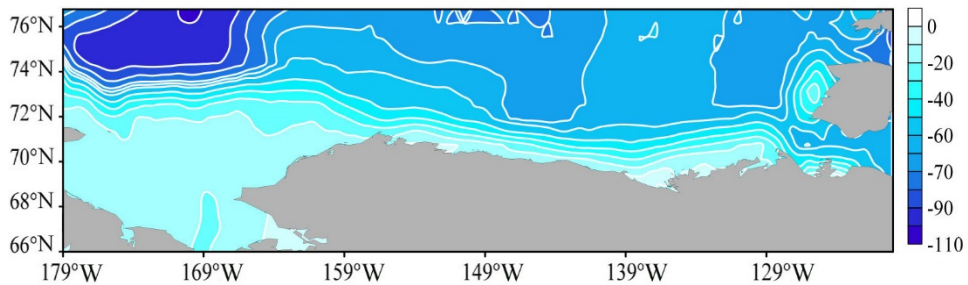


Fig. 14. Average long-term distribution of depth of the maximum amplitude of velocity vertical component of the IW first mode (m) in the Chukchi and Beaufort seas in July, $\lambda = 1000$ m

In the Barents Sea, vertical density gradients are small compared to other Arctic seas. The density transition zone is expressed from July to October [5]. The values of hydrological and wave characteristics averaged over these four months are $N_{\max}(z)_{\text{average}} \sim 10$ cycle/h, $HN_{\max}(z)_{\text{average}} \sim 30$ m, $W_{\max}(z)_{\text{average}} \sim 14$, $HW_{\max}(z)_{\text{average}} \sim 49$ m. Vertical dynamics of waters is most pronounced in winter and spring (December – March) when the seasonal pycnocline is blurred due to convective and wind mixing of waters: $N_{\max}(z)_{\text{average}}$ reaches ~ 4.2 cycle/h, $HN_{\max}(z)_{\text{average}} \sim 60$ m, $W_{\max}(z)_{\text{average}} \sim 34.7$, $HW_{\max}(z)_{\text{average}} \sim 82$ m. In the Kara Sea, the density transition zone persists throughout the year [5]. In June, a seasonal pycnocline, which is clearly

expressed from July to November, begins to form. The characteristics of values averaged over these 5 months are as follows: $N_{\max}(z)_{\text{average}} \sim 30$ cycle/h, $HN_{\max}(z)_{\text{average}} \sim 16$ m, $W_{\max}(z)_{\text{average}} \sim 7.4$, $HW_{\max}(z)_{\text{average}} \sim 31$ m. $W_{\max}(z)$ reaches the highest average values in winter and spring (December – June): $W_{\max}(z)_{\text{average}} \sim 12.5$ at a horizon of ~ 45 m.

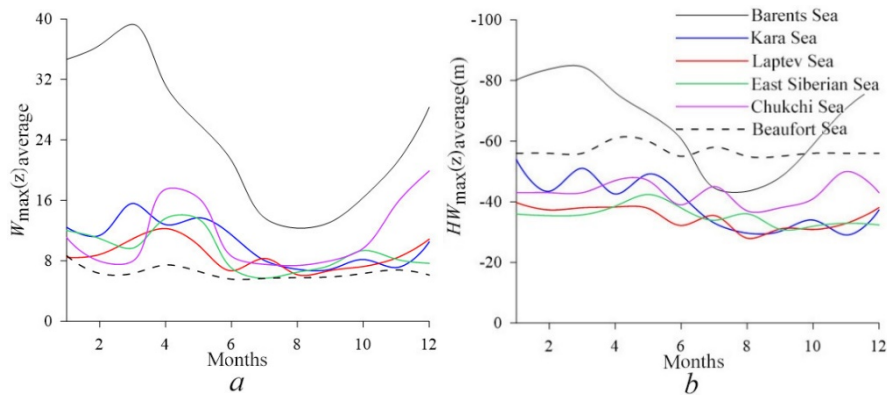


Fig. 15. Intra-annual variation of the sea area average maximum amplitude of velocity vertical component of the IW first mode (conventional units) (a) and its depth (b), $\lambda = 1000$ m

In the Laptev and East Siberian seas, due to the runoff of the Khatanga, Lena, Kolyma, and Indigirka rivers, the pycnocline is also traced throughout the year [6]. In the Laptev Sea from June to November $N_{\max}(z)_{\text{average}}$ is ~ 30 cycle/h, $HN_{\max}(z)_{\text{average}} \sim 16$ m, $W_{\max}(z)_{\text{average}} \sim 7.2$, $HW_{\max}(z)_{\text{average}} \sim 32$ m; in the winter and spring months (December – May) $N_{\max}(z)_{\text{average}} \sim 23.3$ cycle/h, $HN_{\max}(z)_{\text{average}} \sim 17$ m, $W_{\max}(z)_{\text{average}} \sim 10$, $HW_{\max}(z)_{\text{average}} \sim 38$ m. In the East Siberian Sea, the highest $N_{\max}(z)_{\text{average}}$ value is recorded in July and exceeds 45 cycle/h at $HN_{\max}(z)_{\text{average}} \sim 5.5$ m. Accordingly, in July $W_{\max}(z)_{\text{average}}$ is ~ 5.7 , $HW_{\max}(z)_{\text{average}} \sim 34$ m (Fig. 3, 15).

In the Chukchi and Beaufort seas, maximum density gradients are observed in the coastal and marginal areas from June to October [7]. In the Chukchi Sea, stratification is most pronounced in July ($N_{\max}(z)_{\text{average}} \sim 22$ cycle/h, $HN_{\max}(z)_{\text{average}} \sim 13$ m, $W_{\max}(z)_{\text{average}} \sim 7.5$, $HW_{\max}(z)_{\text{average}} \sim 45$ m), in the Beaufort Sea – in June ($N_{\max}(z)_{\text{average}} \sim 42$ cycle/h, $HN_{\max}(z)_{\text{average}} \sim 18$ m, $W_{\max}(z)_{\text{average}} \sim 5.6$, $HW_{\max}(z)_{\text{average}} \sim 55$ m). Wave dynamics is most developed in the mixing zone of summer Pacific waters, desalinated waters of Kotzebue Sound and shelf waters of the Chukchi Sea. In April and December in the Chukchi Sea, the lowest $N_{\max}(z)_{\text{average}}$ values are determined to be ~ 11 cycle/h at $HN_{\max}(z)_{\text{average}} \sim 35$ m and the highest $W_{\max}(z)_{\text{average}}$ values ~ 17 – 19 at $HW_{\max}(z)_{\text{average}} \sim 43$ – 47 m (Fig. 3, 15).

It should be noted that under the considered conditions (density stratification, sea depth, wavelength), the depth of the maximum values of the amplitude of IW velocity vertical component exceeds the depth of the density gradient maximum values by ~ 10 – 20 m. Geographically, areas with small values of maximum buoyancy frequency correspond to areas with large values of the maximum amplitude of IW velocity vertical component. The correlation coefficient between $N_{\max}(z)$ and $W_{\max}(z)$ is within the range from -0.45 to -0.77 , R between the depths $N_{\max}(z)$ and $W_{\max}(z)$ – within the range of 0.23 – 0.78 [8].

Conclusion

Based on *World Ocean Atlas* thermohaline data for 1955–2020 period with a resolution of $0.25^\circ \times 0.25^\circ$, a study of density stratification of waters and IW characteristics in the Barents, Kara, Laptev, East Siberian, Chukchi and Beaufort seas was carried out. An analysis of the relationship between the vertical structure of the density field and the characteristics of free internal waves in these seas was performed.

It is shown that the maximum water stability in the Barents Sea occurs in July – August, in the Kara Sea – in September, November, in the Laptev Sea – in June – November, in the East Siberian and Chukchi seas – in July, in the Beaufort Sea – in June. During these months, the maximum buoyancy frequency values averaged over sea areas are as follows: in the Barents Sea ~ 11 cycle/h, in the Kara Sea ~ 31 cycle/h, in the Laptev Sea ~ 30 cycle/h, in the East Siberian Sea ~ 45 cycle/h, in the Chukchi Sea ~ 22 cycle/h, in the Beaufort Sea ~ 42 cycle/h. The depths of the maximum density gradient averaged over sea areas are as follows: in the Barents Sea ~ 21 m, in the Kara Sea ~ 18 m, in the Laptev Sea ~ 16 m, in the East Siberian Sea ~ 6 m, in the Chukchi Sea ~ 13 m, in the Beaufort Sea ~ 17 m.

It was found that the highest $W_{\max}(z)_{\text{average}}$ values are observed in the months of the lowest density gradients: in the Barents and Kara seas – in March, in the Laptev, East Siberian and Beaufort seas – in April, in the Chukchi sea – in April and December. The correlation coefficient between intra-annual cycles $N_{\max}(z)_{\text{average}}$ and $W_{\max}(z)_{\text{average}}$ lies within the range of $-0.73 \dots -0.95$. The internal waves with the shortest periods (highest frequencies) are observed in the months of maximum density gradients. The correlation coefficient between intra-annual cycles $N_{\max}(z)_{\text{average}}$ and $T_{\text{average}}^{(1)}$ varies within the range of $-0.83 \dots -0.95$.

Under the considered conditions, the depth of the maximum values of the amplitude of IW velocity vertical component exceeds the depth of the density gradient maximum values by approximately 10–20 m.

REFERENCES

1. Rudels, B., Jones, E.P., Schauer, U. and Eriksson, P., 2004. Atlantic Sources of the Arctic Ocean Surface and Halocline Waters. *Polar Research*, 23(2), pp. 181-208. doi:10.3402/polar.v23i2.6278
2. Ivanov, V.V., Frolov, I.E. and Filchuk, K.V., 2020. Transformation of Atlantic Water in the North-Eastern Barents Sea in Winter. *Arctic and Antarctic Research*, 66(3), pp. 246-266. doi:10.30758/0555-2648-2020-66-3-246-266
3. Fedorova, Z.P. and Yankina, Z.S., 1963. The Passage of Pacific Ocean Water through the Bering Strait into the Chukchi Sea. *Okeanologia*, 3(5), pp. 777-784.
4. Bukatov, A.A., Pavlenko, E.A. and Solovei, N.M., 2023. River Runoff Influence on the Density Stratification of the Russian Arctic Seas. In: T. Chaplina, ed., 2023. *Processes in GeoMedia – Volume VI*. Springer Geology. Cham: Springer, pp. 523-536. doi:10.1007/978-3-031-16575-7_47
5. Bukatov, A.A., Pavlenko, E.A. and Solovei, N.M., 2018. Features of Spatial-Time Variability of Väisälä-Brunt Frequency in Barents and Kara Seas. *Processes in GeoMedia*, (3), pp. 1004-1013 (in Russian).

6. Bukatov, A.A., Pavlenko, E.A. and Solovei, N.M., 2019. Regional Features of the Buoyancy Frequency Distribution in the Laptev and East Siberian Seas. *Physical Oceanography*, 26(5), pp. 387-396. doi:10.22449/1573-160X-2019-5-387-396
7. Bukatov, A.E. and Pavlenko, E.A., 2017. The Spatial and Temporal Variability of Distribution of the Buoyancy Frequency in the Chukchi Sea. *Processes in GeoMedia*, 3(12), pp. 573-579 (in Russian).
8. Bukatov, A.A., Solovei, N.M. and Pavlenko, E.A., 2021. Free Short-Period Internal Waves in the Arctic Seas of Russia. *Physical Oceanography*, 28(6), pp. 599-611. doi:10.22449/1573-160X-2021-6-599-611
9. Bukatov, A.A., Solovei, N.M. and Pavlenko, E.A., 2020. Estimation of the Relation between the Dispersion Features of Free Internal Waves and the Density Field Vertical Structure in the Barents and Kara Seas. *Physical Oceanography*, 27(1), pp. 18-27. doi:10.22449/1573-160X-2020-1-18-27
10. Bukatov, A.A., Pavlenko, E.A. and Solovey, N.M., 2021. Influence of Continental Runoff on the Density Stratification of the Laptev and East Siberian Seas. *Processes in GeoMedia*, (2), pp. 1093-1100 (in Russian).
11. Locarnini, R.A., Mishonov, A.V., Baranova, O.K., Boyer, T.P., Zweng, M.M., Garcia, H.E., Reagan, J.R., Seidov, D., Weathers, K.W. [et al.], 2019. *World Ocean Atlas 2018. Volume 1: Temperature*. NOAA Atlas NESDIS 81. Silver Spring, MD: U.S. Department of Commerce, 52 p. Available at: https://www.ncei.noaa.gov/sites/default/files/2021-03/woa18_vol1.pdf [Accessed: 31 October 2021].
12. Zweng, M.M., Reagan, J.R., Seidov, D., Boyer, T.P., Locarnini R.A., Garcia, H.E., Mishonov, A.V., Baranova, O.K., Weathers, K.W. [et al.], 2019. *World Ocean Atlas 2018. Volume 2: Salinity*. NOAA Atlas NESDIS 82. Silver Spring, MD: U.S. Department of Commerce, 50 p. Available at: https://www.ncei.noaa.gov/sites/default/files/2020-04/woa18_vol2.pdf [Accessed: 31 October 2021].
13. Gritsenko, V.A. and Krasitsky, V.P., 1982. On a Method for the Computation of Dispersion Relations and Eigenfunctions for Internal Waves in the Ocean from the Field Measurement Data. *Okeanologia*, (4), pp. 545-549 (in Russian).
14. Kozlov, I.E., Kudryavtsev, V.N. and Sandven, S., 2010. Some Results of Internal Waves Study in the Barents Sea Using Satellite Radar Data. *Problems of Arctic and Antarctic*, (3), pp. 60-69 (in Russian).
15. Zimin, A.V., Romanenkov, D.A., Kozlov, I.E., Chapron, B., Rodionov, A.A., Atadjanova, O.A., Myasoedov, A.G. and Collard, F., 2014. Short Period Internal Waves in the White Sea: Operational Remote Sensing Experiment in Summer 2012. *Issledovanie Zemli iz Kosmosa*, (3), pp. 41-55. doi:10.7868/S0205961414030087 (in Russian).
16. Kozlov, I.E., Kudryavtsev, V.N., Zubkova, E.V., Zimin, A.V. and Chapron, B., 2015. Characteristics of Short-Period Internal Waves in the Kara Sea Inferred from Satellite SAR Data. *Izvestiya, Atmospheric and Oceanic Physics*, 51(9), pp. 1073-1087. doi:10.1134/S0001433815090121
17. Lobovikov, P.V., Kurkina, O.E., Kurkin, A.A. and Kokoulina, M.V., 2019. Transformation of the First Mode Breather of Internal Waves above a Bottom Step in a Three-Layer Fluid. *Izvestiya, Atmospheric and Oceanic Physics*, 55(6), pp. 650-661. doi:10.1134/S0001433819060094
18. Ozhigin, V.K., Ivshin, V.A., Trofimov, A.G., Karsakov, A.L. and Antsiferov, M.Yu., 2016. *The Barents Sea Water: Structure, Circulation, Variability*. Murmansk: PINRO, 260 p. (in Russian).

19. Osadchiev, A.A., 2021. *River Plumes*. Moscow: Scientific World, 286 p. (in Russian).
20. Petrov, K.M., 2008. Principles of Physical-Geographical Differentiation of the Arctic Seas: Kara Sea. *Izvestiya Rossiiskoi Akademii Nauk. Seriya Geograficheskaya*, (6), pp. 19-30 (in Russian).
21. Timofeev, V.T., 1944. [The Barents Sea Sustainability]. *Problems of the Arctic*, (3), pp. 5-37 (in Russian).
22. Ivanov, V.V., Rusanov, V.P., Gordin, O.I. and Osipova, I.V., 1984. Interannual Variability of the Distribution of River Waters in the Kara Sea. *Proceedings of the AARI*, 368, pp. 74-81 (in Russian).
23. Morison, J., Kwok, R., Peralta-Ferriz, C., Alkire, M., Rigor, I., Andersen, R. and Steele, M., 2012. Changing Arctic Ocean Freshwater Pathways. *Nature*, 481, pp. 66-70. doi:10.1038/nature10705
24. Kagan, B.A., Timofeev, A.A. and Sofina, E.V., 2010. Seasonal Variability of Surface and Internal M₂ Tides in the Arctic Ocean. *Izvestiya, Atmospheric and Oceanic Physics*, 46, pp. 652-662. doi:10.1134/S0001433810050105
25. Lavrenov, I.V. and Morozov, E.G., eds., 2002. *Surface and Internal Waves in the Arctic Seas*. Saint Petersburg: Gidrometeoizdat, 362 p. (in Russian).

About the authors:

Anton A. Bukatov, Leading Research Associate, Oceanography Department, Marine Hydrophysical Institute of RAS (2 Kapitanskaya Str., Sevastopol, 299011, Russian Federation), Ph.D. (Phys.-Math.), **ORCID ID: 0000-0002-1165-8428**, **ResearcherID: P-6733-2017**, newisland@list.ru

Nelya M. Solovei, Junior Research Associate, Oceanography Department, Marine Hydrophysical Institute of RAS (2 Kapitanskaya Str., Sevastopol, 299011, Russian Federation), **ORCID ID: 0000-0003-3359-0345**, nele7@mail.ru

Ekaterina A. Pavlenko, Junior Research Associate, Oceanography Department, Marine Hydrophysical Institute of RAS (2 Kapitanskaya Str., Sevastopol, 299011, Russian Federation), **ORCID ID: 0000-0001-9146-5708**, pavlenko.ea@mhi-ras.ru

Contribution of the co-authors:

Anton A. Bukatov – problem statement, research data analysis, analysis and revision of the text

Nelya M. Solovei – development of program algorithms, analysis of the results of numerical experiments, paper correction, literature reviewing

Ekaterina A. Pavlenko – analysis and validation of results, preparation of graphic materials, preparation of the text

The authors have read and approved the final manuscript.

The authors declare that they have no conflict of interest.